Journal of Solid State Chemistry 183 (2010) 2456–2460

Contents lists available at ScienceDirect

Journal of Solid State Chemistry

journal homepage: www.elsevier.com/locate/jssc

Microstructure and electrical–optical properties of cesium tungsten oxides synthesized by solvothermal reaction followed by ammonia annealing

Jing-Xiao Liu [a,b,*], Yoshihiko Ando [a], Xiao-Li Dong [b], Fei Shi [b], Shu Yin [a], Kenji Adachi [c], Takeshi Chonan [c], Akikazu Tanaka [d], Tsugio Sato [a]

[a] Institute of Multidisciplinary Research for Advanced Material, Tohoku University, Sendai 9808577, Japan
[b] School of Chemistry and Materials, Dalian Polytechnic University, Dalian 116034, PR China
[c] Ichikawa Research Laboratory, Sumitomo Metal Mining Co., Ltd, Japan
[d] Technology Division, Advanced Technology Information Department, Sumitomo Metal Mining Co., Japan

ARTICLE INFO

Article history:
Received 12 June 2010
Received in revised form
31 July 2010
Accepted 8 August 2010
Available online 12 August 2010

Keywords:
Cs_xWO_3
Solvothermal reaction
Ammonia annealing
Electrical properties
Optical properties

ABSTRACT

Cesium tungsten oxides (Cs_xWO_3) were synthesized by solvothermal reactions using ethanol and 57.1 vol% ethanol aqueous solution at 200 °C for 12 h, and the effects of post annealing in ammonia atmosphere on the microstructure and electrical–optical properties were investigated. Agglomerated particles consisting of disk-like nanoparticles and nanorods of Cs_xWO_3 were formed in the pure ethanol and ethanol aqueous solutions, respectively. The samples retained the original morphology and crystallinity after annealing in ammonia atmosphere up to 500 °C, while a small amount of nitrogen ion were incorporated in the lattice. The as-prepared Cs_xWO_3 sample showed excellent near infrared (NIR) light shielding ability as well as high transparency in the visible light region. The electrical resistivity of the pressed pellets of the powders prepared in pure ethanol and 57.1 vol% ethanol aqueous solution greatly decreased after ammonia annealing at 500 °C, i.e., from 734 to 31.5 and 231 to 3.58 Ω cm, respectively.

1. Introduction

In recent years, tungsten bronzes have attracted much attention due to their interesting electro-optic, photochromic and superconducting properties [1–7]. Particularly, tungsten bronzes M_xWO_3 with doping small ions such as H^+, Ag^+, Li^+, Na^+, K^+ and Cs^+ into WO_3 have better optical and electrical properties [8–14]. It has been reported that the tungsten bronzes with the hexagonal phase are of particular interest in the application of electrochromic devices owing to the relatively high diffusion coefficients of hydrogen ions and metal ions compared with those of the orthorhombic phase and pure WO_3 [15]. As for the Cs-doped WO_3, the superconductivity of Cs_xWO_3 prepared by the thermal vapor growth process has been studied [16,17]. It was reported that Cs_xWO_3 with $0.3 \geq x \geq 0.19$ was a 3D superconductor, a transition from a metal to an insulator occurs at $x < 0.19$, and a 2D superconductor was formed at $x = 0.05$ [17]. In addition, the hexagonal tungsten bronze (HTB) phase of $Cs_{0.33}WO_3$ was regarded as being highly attractive in solar filter applications because of its strong absorption in the near-infrared (NIR) wavelengths [18].

The traditional methods for preparing the hexagonal tungsten bronze Cs_xWO_3 usually require high temperature and harsh reaction conditions, such as heating mixtures of WO_3 with K, Rb or Cs salts in reducing atmospheres at 1000 °C. Recently, morphology and phase control of particles by soft chemical synthesis methods have attracted wide interest in the synthesis of many oxides such as ZnO [19,20], WO_3 [21–25], etc. It has been acknowledged that the microstructure and morphology of particles play an important role in its properties. Up to now, synthesizing pure WO_3 with different morphologies and properties has been widely reported [26–29]. However, there is limited work reported on the synthesis and characterization of Cs_xWO_3 with controlled morphology by solvothermal reaction. Furthermore, the effects of ammonia annealing on the microstructure and electrical–optical properties of Cs_xWO_3 have not been reported. Therefore, in this present study, the microstructure, morphology and electrical–optical properties of Cs_xWO_3 synthesized by solvothermal reaction followed by ammonia annealing were investigated systematically.

2. Experimental

2.1. Sample preparation

Tungsten hexachloride (WCl_6) and cesium hydroxide monohydrate ($CsOH \cdot H_2O$) were used as raw materials and pure ethanol

* Corresponding author at: Dalian Polytechnic University, School of Chemistry and Materials, Dalian 116034, China. Fax: +86 411 86323736.
E-mail addresses: jxiaoliu@sina.com, drliu-shi@dlpu.edu.cn (J.-X. Liu).

0022-4596/$ - see front matter Crown Copyright © 2010 Published by Elsevier Inc. All rights reserved.
doi:10.1016/j.jssc.2010.08.017

(purity 99.5%) and 57.1 vol% ethanol aqueous solution were used as the solvothermal reaction solvents, where the initial concentration of tungsten hexachloride in each reaction solution and the atomic ratio of Cs/W were adjusted to be 0.14 M and 0.33, respectively. After transferring the reaction solution into a Teflon®-lined autoclave of 100 ml of internal volume, the autoclave was heated at 200 °C for 12 h in an electric oven. The reaction using the pure ethanol solvent was conducted without rolling, while when using the 57.1 vol% ethanol aqueous solution, the autoclave was rotated at the rolling speed of 100 rpm in order to depress excess grain growth. The obtained solid precipitates were then centrifuged and washed with ethanol three times followed by vacuum drying at 60 °C overnight. The TG-DTA analysis showed that only a 0.2% weight loss occurred from 24 to 500 °C, indicating that less amounts of water and organic molecules were adsorbed on the sample.

Ammonia annealing was conducted in a tubular furnace at 300 or 500 °C for 1 h with the flow of ammonia at 400 ml/min.

2.2. Characterization

The morphology and microstructures of the samples were observed by scanning electron microscopy (SEM, HITACHI S-4800) and transmission electron microscopy (TEM, JEOL JEM-2010). The surface composition of the samples and the binding energies of W, Cs, O and N in the samples were determined by X-ray photoelectron spectroscopy (XPS, Pekin Elmer PHI 5600). The phase compositions of the samples were determined by X-ray diffraction analysis (XRD, Shimadzu XD-D1) using graphite-monochromized Cu$K\alpha$ radiation. The contents of N incorporated in the sample after ammonia annealing were analyzed by the XPS analysis and thermal conductivity analysis using oxygen–nitrogen analyzer (HORIBA, MGA-2800).

The electrical resistivity of the samples before and after ammonia annealing at 500 °C for 1 h was measured by a four-probe method (Mitsubishi Chemical Corporation, Lolestra-GP MIP-T610). First, the powder samples before and after ammonia annealing at 500 °C were pressed into disks of $\phi 8 \times 1\ mm^2$ at 200 MPa for electrical resistivity measurement. Three disks of $\phi 8 \times 1\ mm^2$ were prepared for every sample, and then measurements were performed three times for every disk. The average value calculated from the nine readings for every sample was noted as the final electrical resistivity result.

The optical properties were evaluated by measuring the ultraviolet/visible/near-infrared transmittance spectra of thin films of the sample powders dispersed on a quartz glass by a

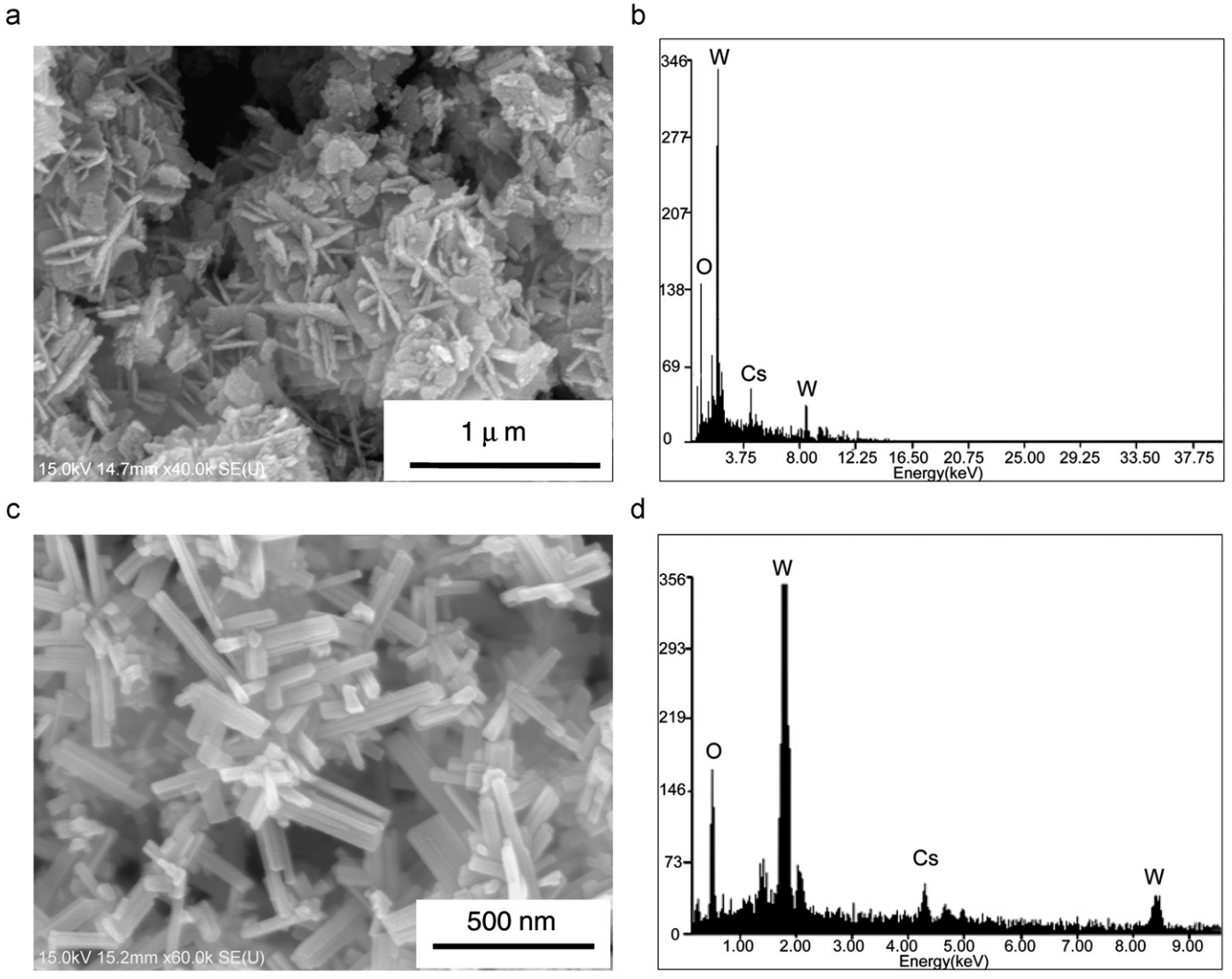

Fig. 1. SEM images of (a) the sample prepared in ethanol and (b) the EDAX mapping analysis patterns of the sample (a), and (c) the sample prepared in the 57.1 vol% ethanol aqueous solution, and (d) the EDAX mapping analysis patterns of the sample (c).

spectrophotometer (JASCO V-670 spectrophotometer), where the sample powders were dispersed in a media agitation mill to reduce the grain size using yttria doped tetragonal zirconia beads, polymer dispersing agents and toluene.

3. Results and discussion

3.1. Effects of the solvents on the microstructure and properties

Fig. 1 shows the typical SEM images of the as-prepared products. It can be seen that the agglomerated particles consisted of disk-like particles of 0.1–0.5 μm in diameter were formed in ethanol. In contrast, for the sample synthesized in the 57.1 vol% ethanol aqueous solution, micrometer sized aggregated particles consisting of needles of ca. 200–500 nm length were formed. The EDAX spectra of the samples obtained in the ethanol and 57.1 vol% ethanol aqueous solution clearly indicated peaks corresponding to W and Cs (Fig. 1(b) and (d)), suggesting the formation of Cs_xWO_3.

Fig. 2 displays the W_{4f} and Cs_{3d} XPS spectra of the samples synthesized with the pure ethanol and 57.1 vol% ethanol aqueous solution. From the W_{4f} XPS spectra, it can be seen that both samples exhibited two principal peaks at 35.9/38.0 and 36.1/38.0 eV, respectively. The surface compositions of the products determined from the ratio of the O_{1s}, W_{4f} and Cs_{3d} peak intensities were $Cs_{0.292}WO_{3.107}$ and $Cs_{0.213}WO_{3.08}$, respectively. The difference in the amount of Cs entered into the lattice might be due to the difference in the reduction potential of the reaction atmosphere, i.e., the pure ethanol provided stronger reduction atmosphere than the water/ethanol mixed solvent.

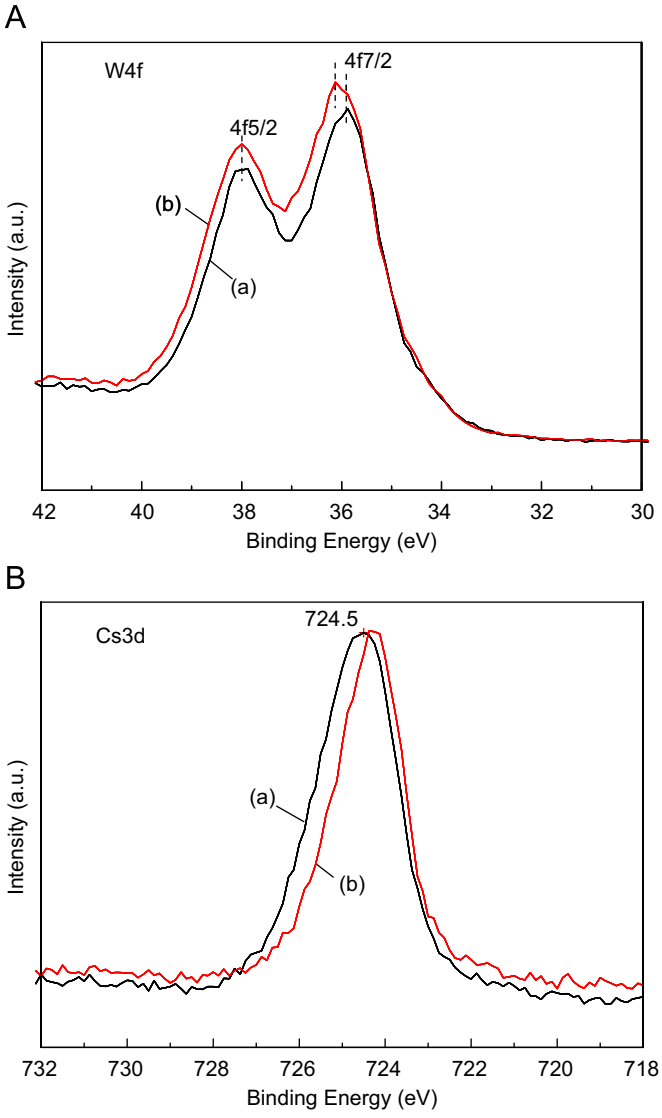

Fig. 2. W_{4f} and Cs_{3d} XPS spectra of Cs_xWO_3 prepared by the solvothermal reactions in (a) ethanol and (b) the 57.1 vol% ethanol aqueous solution at 200 °C for 12 h.

The XRD patterns of the products are shown in Fig. 3. The XRD pattern of the product synthesized in ethanol agreed well with that of hexagonal $Cs_{0.3}WO_3$ with the lattice constants $a=7.4154$, $c=7.6062$ (JCPDS 81-1244, standard values $a=7.404$, $c=7.609$). It was reported that the large Cs ions (0.170 nm) could fit better in the hexagonal vacant tunnels (0.163 nm) in the hexagonal tungsten bronze structure rather than in the rectangular vacant tunnels in the cubic tungsten bronze structure [18]. In contrast, the XRD pattern of the sample synthesized in the 57.1 vol% ethanol aqueous solution agreed well with the standard XRD pattern of hexagonal $Cs_{0.20}WO_3$ with the lattice constants of $a=7.4162$ and $c=7.5762$ (JCPDS 83-1333, standard values $a=7.420$, $c=7.567$). Although the XRD pattern of $Cs_{0.20}WO_3$ (JCPDS 83-1333) was very similar with that of $Cs_{0.3}WO_3$ (JCPDS 81-1244), according to the XPS results in Fig. 3, the crystal phase in the sample synthesized in the 57.1 vol% ethanol aqueous solution is more likely to have been $Cs_{0.2}WO_3$.

3.2. Effects of ammonia annealing

With the aim of improving the optical and electrical properties of Cs_xWO_3, the as-prepared Cs_xWO_3 samples were annealed in an

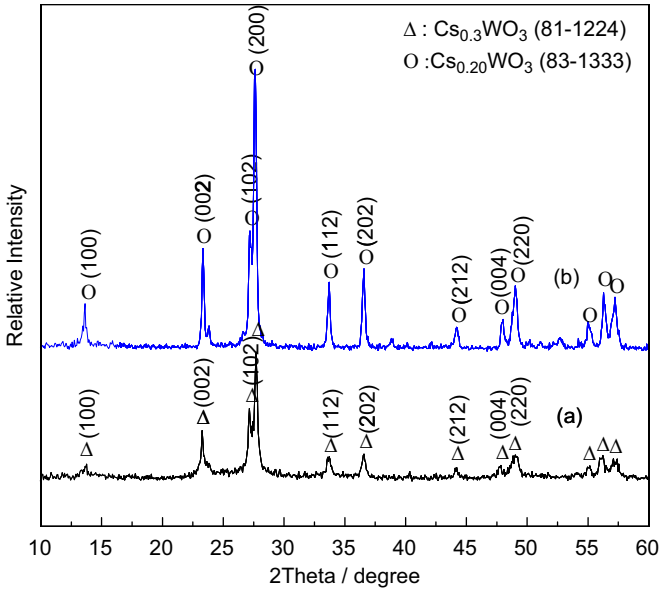

Fig. 3. The XRD patterns of Cs_xWO_3 prepared by the solvothermal reactions in (a) ethanol and (b) the 57.1 vol% ethanol aqueous solution at 200 °C for 12 h.

Table 1
The electrical resistivities of Cs_xWO_3 before and after ammonia annealing at 500 °C for 1 h.

Reaction solvent	Electrical resistivities (Ω cm)	
	Before NH_3 annealing	After NH_3 annealing
Pure ethanol	734	31.5
57.1 vol% ethanol aqueous solution	231	3.58

ammonia gas atmosphere at 300 and 500 °C for 1 h, respectively. It was found that ammonia annealing resulted in no noticeable changes in the morphology and crystallinity of the samples up to 500 °C, but it resulted in decrease in the electrical resistivity. Table 1 shows the electrical resistivity of the pressed powder pellets of Cs_xWO_3 formed in pure ethanol and 57.1 vol% ethanol aqueous solution before and after ammonia annealing at 500 °C for 1 h. The electrical resistivity of the as-prepared Cs_xWO_3 in ethanol and 57.1 vol% ethanol aqueous solution were 7.34×10^2 and $2.31 \times 10^2\ \Omega$ cm, and those after ammonia annealing greatly decreased to 3.15×10^1 and $3.58 \times 10^0\ \Omega$ cm, respectively, (i.e., an one or two order of magnitude decrease in electrical resistivity), although no noticeable changes were observed in the microstructures by SEM observations and XRD profiles of the samples. Therefore, this may be due to the elimination of the impurities adsorbed on the surface, homogenization of the chemical composition, increase in the carrier concentration by the reduction of W^{6+}–W^{5+}, and incorporation of nitrogen ions in the lattice. Similar results were reported that both nitrogen-doped tungsten oxide nanowires by treating in ammonia gas [30] and the nitrogen-doped tungsten oxide thin films prepared at P_{N_2} of 0.12 mbar exhibited lower resistivity than undoped tungsten oxide [31].

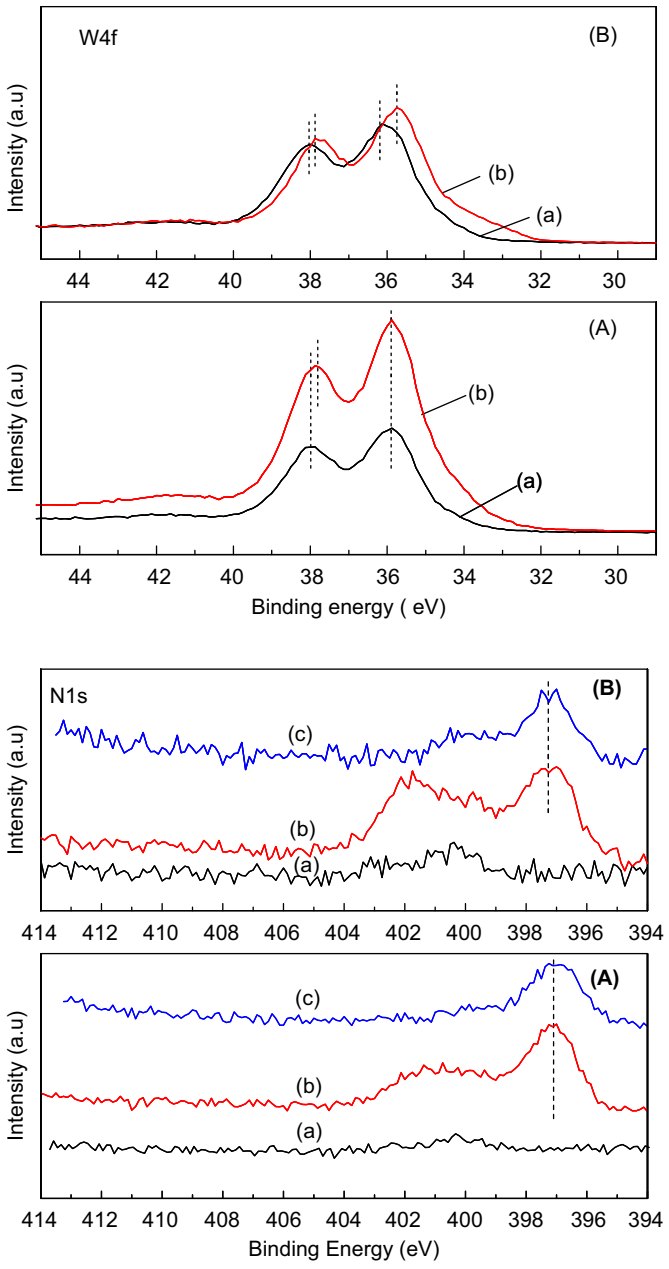

Fig. 4. The W_{4f} and N_{1s} XPS profiles of Cs_xWO_3 synthesized in (A) ethanol and (B) the 57.1 vol% ethanol aqueous solution (a) before ammonia annealing, (b) after ammonia annealing at 500 °C for 1 h and (c) after Ar spattering of sample (b).

Fig. 4 shows the W_{4f} and N_{1s} XPS spectra of the samples before and after ammonia annealing at 500 °C for 1 h. It can be seen that the two peaks in the W_{4f} XPS spectra showed a red shift after ammonia annealing, which indicates that the chemical state of W was changed due to the partial reduction of W^{6+} and/or incorporation of nitrogen in the lattice by the NH_3 annealing. As for the N_{1s} spectra, the peaks of N1*s* around 397 and 401 eV appeared in both samples after ammonia annealing at 500 °C. Since the peak intensities around 401 eV decreased after Ar spattering, this peak seems to be attributed to nitrogen adsorbed on the surface.

Table 2 displays the results of elemental analyses of the products by XPS. It can be seen that the content of O decreased and that of N increased after ammonia annealing, indicating the incorporation of nitrogen ions. The atomic ratios of O/W and (O+N)/W were higher than 3, especially after ammonia annealing. This might be due to the adsorption of oxygen and ammonia on the surface of the particle. Additionally, it was found that the Cs/W atomic ratio decreased a little after ammonia annealing. This might be due to the diffusion of Cs ions from the surface to the inside the particle since XPS is a surface sensitive technique, i.e., the Cs ions content on the surface region of the as-prepared samples were higher than that inside. These results suggest that thermal treatment at 500 °C is useful to homogenize the chemical composition of particles.

The nitrogen content in the samples annealed in NH_3 atmosphere at 300 and 500 °C are shown in Table 3, where the values were determined by a thermal conductivity analysis. It is obvious that the N element content increased with an increase in the ammonia annealing temperature. The contents of N element in Cs_xWO_3 prepared in pure ethanol and 57.1 vol% ethanol solution followed by ammonia annealing at 300 and 500 °C were determined to be 0.23 and 1.22 mass%, and 0.57 and 1.51 mass%, respectively. These values are lower than those determined by XPS analysis. This may be due to the fact that XPS analysis is a

Table 2
Element analysis results by the XPS method.

Solvent	Sample	Element content (atomic% (mass%))				O/W or (O+N)/W atomic ratio	Cs/W atomic ratio
		N	O	Cs	W		
Pure ethanol	Before ammonia annealing	–	70.6	6.63	22.7	3.11	0.29
	After ammonia annealing	7.59 (1.8)	64.3 (17.1)	5.69 (12.6)	22.4 (68.5)	3.22	0.25
57.1 vol% ethanol aqueous solution	Before ammonia annealing	–	71.7	4.96	23.3	3.08	0.21
	After ammonia annealing	11 (2.6)	62.4 (17.1)	4.07 (9.26)	22.56 (71.0)	3.25	0.18

Table 3
Nitrogen contents (mass%) determined by the thermal conductivity analysis.

Solvent	NH_3 anneal temperature (°C)	
	300	500
Pure ethanol	0.23	1.22
57.1 vol% ethanol aqueous solution	0.57	1.51

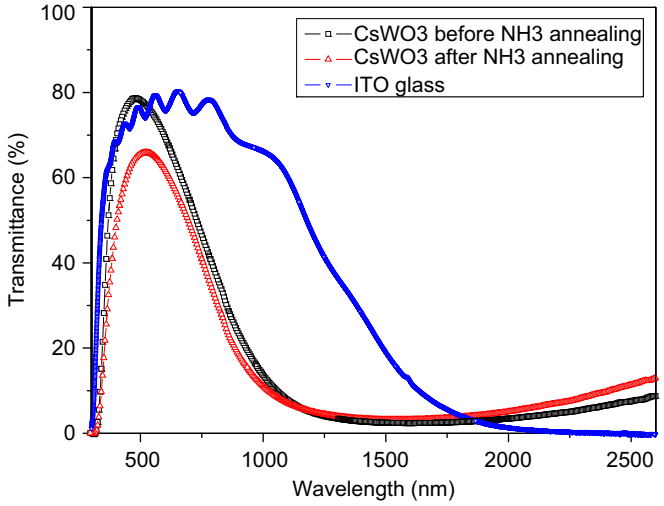

Fig. 5. UV–vis–near infrared diffuse transmittance spectra of ITO glass and $Cs_{0.3}WO_3$ synthesized in the 57.1 vol% ethanol aqueous solution before and after annealing in NH_3 gas atmosphere at 500 °C for 1 h.

surface sensitive technique and tends to show higher values for adsorbed species.

Fig. 5 shows the UV–vis–NIR transmittance spectra of the thin film of Cs_xWO_3 formed in the 57.1 vol% ethanol aqueous solution before and after ammonia annealing. The UV–vis–IR diffuse transmittance spectrum of indium tin oxides (ITO) glass is also presented in Fig. 5 as a reference datum. It can be seen that the as-prepared sample showed excellent near infrared (NIR) shielding ability as well as high transparency in the visible light region, and the NIR shielding ability of the as-prepared Cs_xWO_3 sample is higher than the ITO glass. This result indicates that the as-prepared Cs_xWO_3 is an ideal heat shielding material which can replace ITO. It is also seen that the ammonia annealing resulted in no noticeable change in NIR shielding degree, but decreased the transparency in the visible light region to some extent. This may be probably due to the formation of an anion vacancy for the charge compensation corresponding to the incorporation of nitrogen ions.

4. Conclusion

Cesium tungsten oxides, Cs_xWO_3, were prepared by solvothermal reactions at 200 °C for 12 h using ethanol and a water/ethanol mixed solvent. The solvothermal reaction solvents played an important role for the control of the morphology and microstructure of Cs_xWO_3, i.e., agglomerated particles consisting of disk-like nanoparticles of $Cs_{0.3}WO_3$ and nanorods of $Cs_{0.2}WO_3$ were formed in pure ethanol and the water/ethanol mixed solvent, respectively. Ammonia annealing resulted in no noticeable changes in the morphology and crystallinity of the samples up to 500 °C, although it did result in the incorporations of nitrogen ions in the lattice of Cs_xWO_3 as well as a decrease in the electric resistivity and visible light transparency.

Acknowledgments

This work was supported by the Ministry of Education, Culture, Sports, Science and Technology, Japan, Special Education and Research Expenses on "Post-Silicon Materials and Devices Research Alliance".

References

[1] C.H. Rüscher, K.R. Dey, T. Debnath, I. Horn, R.G.A. Hussain, J. Solid State Chem. 181 (2008) 90.
[2] F. Krumeich, R. Nesper, J. Solid State Chem. 179 (2006) 1857.
[3] J. Guo, C. Dong, L. Yang, G. Fu, H. Chen, Mater. Res. Bull. 41 (2006) 655.
[4] F.J. Castro, F. Tonus, J.-L. Bobet, G. Urretavizcaya, J. Alloys Compd. 495 (2010) 537.
[5] G. Urretavizcaya, F. Tonus, E. Gaudin, J.-L. Bobet, F.J. Castro, J. Solid State Chem. 180 (2007) 2785.
[6] J. Guo, C. Dong, L. Yang, G. Fu, H. Chen, Mater. Res. Bull. 42 (2007) 1384.
[7] K.R. Dey, C.H. Rüscher, Th.M. Gesing, A. Hussain, Mater. Res. Bull. 42 (2007) 591.
[8] H. Kamal, A.A. Akl, K. Abdel-Hady, Physica B 349 (2004) 192.
[9] L. Chen, S.C. Tsang, Sensors Actuators B 89 (2003) 68.
[10] L. Berggren, J. Ederth, G.A. Niklasson, Sol. Energy Sol. Cells 84 (2004) 329.
[11] R. Azimirad, M. Goudarzi, O. Akhavan, A.Z. Moshfegh, Vacuum 82 (2008) 821.
[12] S. Raj, D. Hashimoto, H. Matsui, S. Souma, T. Sato, T. Takahashi, S. Ray, A. Chakraborty, D.D. Sarma, P. Mahadevan, S. Oishi, W.H. McCarroll, M. Greenblatt, J. Magn. Magn. Mater. 310 (2007) e231.
[13] Z. Gu, Y. Ma, T. Zhai, B. Gao, W. Yang, J. Yao, Chem. Eur. J 12 (2006) 7717.
[14] J. Guo, C. Dong, L. Yang, H. Chen, Mater. Res. Bull. 43 (2008) 779.
[15] Q. Zhong, K. Colbow, Thin Solid Films 196 (1991) 305.
[16] G. Leitus, H. Cohen, S. Reich, Physica C 371 (2002) 321.
[17] Z. Barkay, E. Grunbaum, G. Leitus, S. Reich, J. Supercond. Nov. Magn. 21 (2008) 145.
[18] H. Takeda, K. Adachi, J. Am. Ceram. Soc. 90 (2007) 4059.
[19] T. Long, K. Takabatake, S. Yin, T. Sato, J. Cryst. Growth 311 (2009) 576.
[20] M.S. Akhtar, M.A. Khan, M.S. Jeon, O.-B. Yang, Electrochim. Acta 53 (2008) 7869.
[21] M. Gillet, R. Delamare, E. Gillet, Appl. Surf. Sci. 254 (2007) 270.
[22] J.-H. Ha, P. Muralidharan, D.K. Kim, J. Alloys Compd. 475 (2009) 446.
[23] Z. Gu, T. Zhai, B. Gao, X. Sheng, Y. Wang, H. Fu, Y. Ma, J. Yao, J. Phys. Chem. B 110 (2006) 23829.
[24] Y. Baek, K. Yong, J. Phys. Chem. C 111 (2007) 1213.
[25] H.G. Choi, Y.H. Jung, D.K. Kim, J. Am. Ceram. Soc. 88 (2005) 1684.
[26] Z.-G. Zhao, M. Miyauchi, J. Phys. Chem. C 113 (2009) 6539.
[27] K. Huang, Q. Pan, F. Yang, S. Ni, X. Wei, D. He, J. Phys. D: Appl. Phys. 41 (2008) 155417.
[28] Y. Baek, K. Yong, J. Phys. Chem. C 111 (2007) 1213.
[29] X.C. Song, Y.F. Zheng, E. Yang, Y. Wang, Mater. Lett. 61 (2007) 3904.
[30] M.-T. Chang, L.-J. Chou, Y.-L. Chueh, Y.-C. Lee, C.-H. Hisieh, C.-D. Chen, Y.-W. Lan, L.-J. Chen, Small 3 (2007) 658.
[31] K.J. Lethy, S. Potdar, V.P. Mahadevan Pillai, V. Ganesan, J. Phys. D: Appl. Phys. 42 (2009) 095412.